Cell Stem Cell
Article

Syndecan-4-Expressing Muscle Progenitor Cells in the SP Engraft as Satellite Cells during Muscle Regeneration

Kathleen Kelly Tanaka,[1] John K. Hall,[1] Andrew A. Troy,[1] D.D.W. Cornelison,[2] Susan M. Majka,[3] and Bradley B. Olwin[1,*]
[1]MCD Biology, University of Colorado, Boulder, CO 80309, USA
[2]Biological Sciences and Bond Life Sciences Center, University of Missouri, Columbia, MO 65211, USA
[3]Department of Medicine/Cardiology, University of Colorado Health Sciences Center, Aurora, CO 80045, USA
*Correspondence: bradley.olwin@colorado.edu
DOI 10.1016/j.stem.2009.01.016

SUMMARY

Skeletal muscle satellite cells, located between the basal lamina and plasma membrane of myofibers, are required for skeletal muscle regeneration. The capacity of satellite cells as well as other cell lineages including mesoangioblasts, mesenchymal stem cells, and side population (SP) cells to contribute to muscle regeneration has complicated the identification of a satellite stem cell. We have characterized a rare subset of the muscle SP that efficiently engrafts into the host satellite cell niche when transplanted into regenerating muscle, providing 75% of the satellite cell population and 30% of the myonuclear population, respectively. These cells are found in the satellite cell position, adhere to isolated myofibers, and spontaneously undergo myogenesis in culture. We propose that this subset of SP cells (satellite-SP cells), characterized by ABCG2, Syndecan-4, and Pax7 expression, constitutes a self-renewing muscle stem cell capable of generating both satellite cells and their myonuclear progeny in vivo.

INTRODUCTION

Maintenance and repair of skeletal muscle tissue is essential for survival of locomotor organisms. Although satellite cells are thought to be the primary source of new myonuclei during skeletal muscle growth and repair, the engraftment capability of isolated satellite cells into injured or diseased skeletal muscle is poor (Asakura et al., 2007; Montarras et al., 2005; Beauchamp et al., 1999). Indeed, cells derived from other sources including mesoangioblasts (Sampaolesi et al., 2003, 2006), pericytes (Dellavalle et al., 2007), and bone marrow stem cells (Gussoni et al., 1999; LaBarge and Blau, 2002) engraft into myofibers with greater efficiency than isolated satellite cells. Only a subset of muscle cells enriched for CD34 expression by cell sorting is capable of engraftment into skeletal muscle myofibers and into the host satellite cell niche (Montarras et al., 2005; Cerletti et al., 2008; Sacco et al., 2008). Although efficient at myonuclear engraftment, these cells engraft with much lower frequencies into the satellite cell niche. These observations, together with data demonstrating asymmetric division of satellite cells (Kuang et al., 2007) and satellite cell heterogeneity (Olguin and Olwin, 2004; Zammit et al., 2004), suggest that a rare population of satellite cells may exist with enhanced stem cell-like characteristics.

Many adult tissues, including bone marrow (Goodell et al., 1996), heart (Asakura et al., 2002), lung (Majka et al., 2005), and skeletal muscle (Majka et al., 2003), possess cells that exhibit the SP phenotype. Indeed, the discovery of these cells in skeletal muscle and their myogenic potential suggested they may function as satellite cell progenitors; however, the low efficiency of muscle SP cell engraftment into skeletal muscle suggested that this population was not representative of a skeletal muscle progenitor (Muskiewicz et al., 2005). Here, we show that a subset of the muscle SP cells that possess both SP and satellite cell characteristics function as efficient satellite cell progenitors. Although the majority of SP cells reside in the interstitium (Meeson et al., 2004), satellite-SP cells (1) can be found in the satellite cell position, (2) remain associated with isolated myofibers, (3) spontaneously fuse in culture, and (4) generate satellite cell progeny in vivo, all characteristics consistent with a satellite cell progenitor. Evidence that a subpopulation of satellite cells may function as a reserve or progenitor population was described using in vivo labeling techniques more than three decades ago (reviewed in Schultz, 1996). Recently, the demonstrations of satellite cell heterogeneity (Olguin and Olwin, 2004; Zammit et al., 2004), coupled with identity of a small population of satellite cells that exhibits asymmetric cell division (Kuang et al., 2007), and long-term BrdU retention (Shinin et al., 2006), all characteristics of stem cells, have further strengthened this idea.

RESULTS

Skeletal Muscle SP Cells Express Syndecan-3 and Syndecan-4

When examining data from microarray analyses of Syndecan-3+/Syndecan-4+ cells isolated by fluorescence-activated cell sorting (FACS) from uninjured muscle, we found high-level expression of both *Abcg2* and *Cd34*. This expression is dramatically reduced in cells sorted from $BaCl_2$-injured muscles, 24 hr postinjury (Figure 1A, and see Table S1 available online). The high-level expression of these cell markers, coupled with their differential expression following injury, prompted us to examine ABCG2 and CD34 protein expression in the satellite cell population. Although others have successfully observed CD34 immunoreactivity in

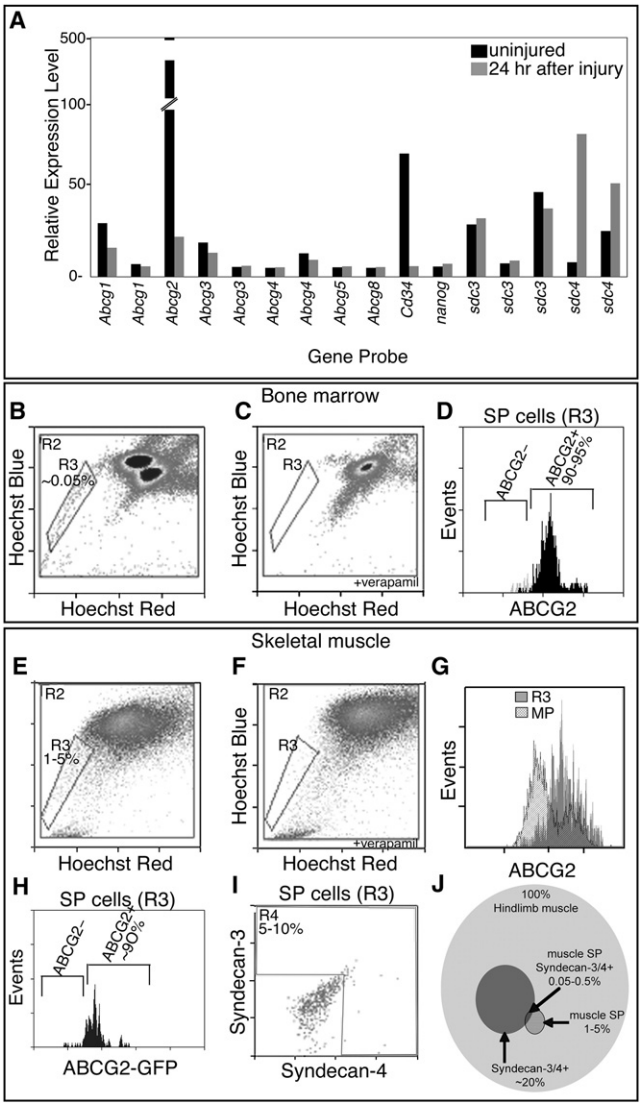

Figure 1. A Subset of Skeletal Muscle SP Cells Expresses the Satellite Cell Markers Syndecan-4 and Syndecan-3

Relative expression levels of genes obtained from microarray data from FACS-purified Syndecan-3+/Syndecan-4+ satellite cells isolated from uninjured muscles (black) and muscles 24 hr after $BaCl_2$ injury (gray) and filtered for selected stem cell genes: the *Abcg* family, *Cd34*, *nanog*, and the satellite cell-specific genes *sdc3* and *sdc4* ([A], probe sets ordered 5′ to 3′). Live-cell FACS profiles for bone marrow-derived cells (B–D) and skeletal muscle-derived cells (E–I) incubated with Hoescht 33342 in the presence (C and F) and absence (B, D, E, and G–I) of verapamil to identify the SP gate (R3 regions with cell percentages noted). More than 90% of SP cells from both tissues express the ABCG2 transporter (D and G), gray histogram with ABCG2 antibody, and (H) using the *Abcg2/GFP* mouse (Tadjali et al., 2006), while the majority of main population cells located above the SP gate do not express ABCG2 ([G], hatched histogram). A subpopulation of muscle SP cells also expresses the satellite cell markers Syndecan-4 and Syndecan-3 ([I], R4 region) as identified by costaining with antibodies during SP profiling. (J) A Venn diagram depicting the percent of Syndecan-3+/Syndecan-4+ muscle SP cells within the cohort of all cells in the entire hindlimb muscle tissue and within the context of muscle SP cells. Percentages of individual cell populations are noted. Background gates were set with less than 0.5% of controls scored as positive.

satellite cells, in our hands the staining patterns were highly variable and inconsistent (data not shown), and thus we focused on ABCG2.

ABCG2 is the ATP-binding cassette transporter responsible for the majority of the SP phenotype originally characterized in bone marrow (Goodell et al., 1996; Zhou et al., 2001). Therefore, we asked if skeletal muscle cells expressing Syndecan-4, which marks all Pax7+ and c-met+ satellite cells (Cornelison et al., 2001; Brack et al., 2007; Bosnakovski et al., 2008), also express ABCG2 protein using an anti-ABCG2 antibody. First, to verify that the anti-ABCG2 antibody identifies cells exhibiting the SP phenotype, we performed FACS analysis of bone marrow cells using Hoechst 33342 dye efflux to identify SP cells (R3 in Figures 1B and 1C) and compared the SP cells identified by dye efflux with those identified by anti-ABCG2 immunoreactivity. ABCG2 immunoreactive cells comprised 90%–95% of the SP cell population, confirming the utility of the ABCG2 antibody for identifying SP cells (Figure 1D). Although the majority of bone marrow SP cells are ABCG2+, multiple ABC transporters contribute to the SP phenotype, and thus the entire SP is not ABCG2 immunoreactive (Zhou et al., 2001). In hindlimb skeletal muscle, we identified SP cells by dye efflux that comprised 1%–5% of total hindlimb cells (Figures 1E and 1F, R3 region), similar to that reported by others (Montanaro et al., 2004). The majority (90%) of these SP cells are ABCG2 immunoreactive (Figure 1G, gray). To further verify the utility of the ABCG2 antibody, we examined cells located above the SP gate in the main population, which are generally not ABCG2 immunoreactive (Figure 1G, hatched). Finally, we isolated SP cells using Hoescht dye exclusion from a mouse expressing GFP from an IRES-GFP knocked into the third intron of the *Abcg2* locus (Tadjali et al., 2006). These cells are both GFP+ and anti-GFP immunoreactive, confirming that the anti-ABCG2 antibody recognizes cells expressing *Abcg2* (Figure 1H). We then examined muscle SP cells isolated by dye exclusion for satellite cell markers by FACS and found that 5%–10% of hindlimb SP cells are immunoreactive for the satellite cell markers Syndecan-3 and Syndecan-4 (Figure 1I). This subset of hindlimb cells represented in the Venn diagram is a subfraction of the SP that expresses the satellite cell marker Syndecan-4 (Figure 1J). To allow detection of additional markers and to alleviate the damaging effects of the Hoescht 33342 dye, we used anti-ABGG2 immunoreactivity to identify and isolate muscle SP cells except where noted.

A Subset of Satellite Cells Is SP Cells

To further characterize the Syndecan-3+/Syndecan-4+ SP cells, we analyzed mononuclear cells from mouse hindlimb muscle tissue by FACS using the anti-ABCG2 antibody. Of the entire population of mononuclear cells in the hindlimb (Figure 2A), 10%–20% are Syndecan-4 immunoreactive (Figure 2B), and all Syndecan-4+ cells are viable (Figure 2C). To verify that these cells are not significantly contaminated by cells from the blood and endothelial lineages, we profiled for CD45, Gr-1, Mac-1, Thy-1, and PECAM-1. The blood cell markers were not expressed by Syndecan-4+ cells isolated from skeletal muscle (Figures 2D–2G). Prior reports suggest that satellite cells as well as endothelial cells express PECAM-1 (CD31) (De Angelis et al., 1999), and we found a similar small percentage of Syndecan-4+ cells (7% of all Syndecan-4+ cells) and Syndecan-4+/ABCG2+ cells

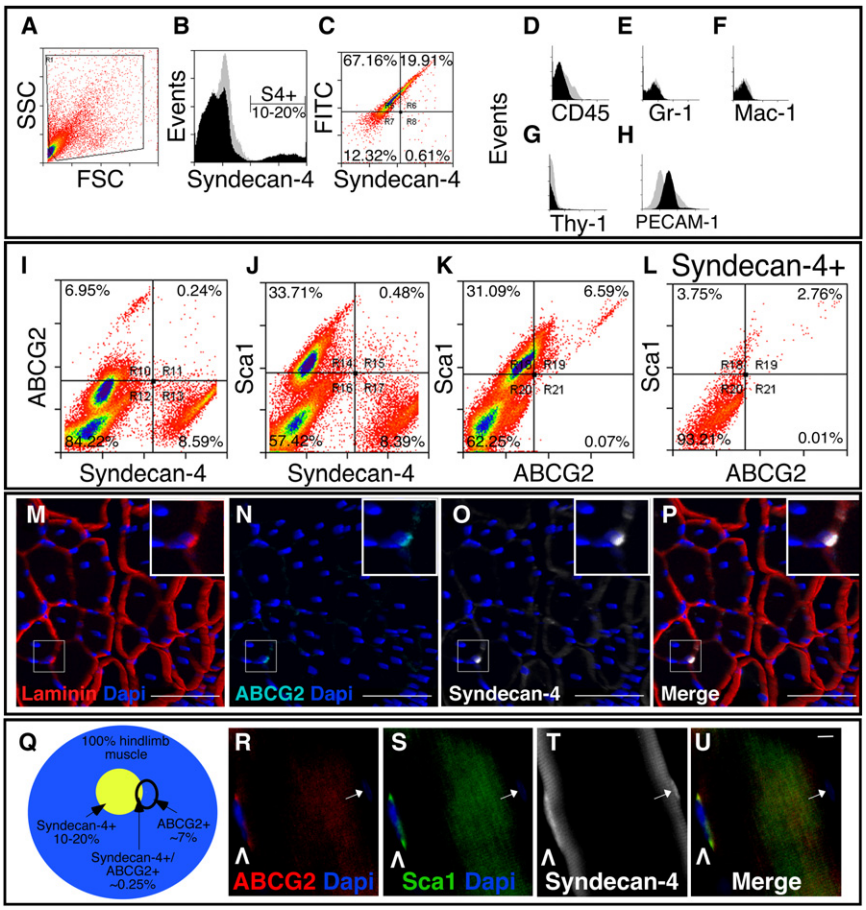

Figure 2. Satellite-SP Cells Express the Stem Cell Markers ABCG2 and Sca1

Live-cell FACS profiles for hindlimb skeletal muscle (A–L) identify a population of Syndecan-4+ satellite cells in the total events ([A], FSC/forward scatter and SSC/side scatter), plotted as events versus Syndecan-4 fluorescence intensity to resolve Syndecan-4+ cells ([B], black profile) from background ([B], gray profile). Live cells convert fluorescein diacetate to FITC, showing the majority of Syndecan-4+ cells are viable ([C], region R6). Syndecan-4+ cells are negative for the blood linage makers CD45 (D), Gr-1 (E), Mac-1 (F), and Thy-1 (G), and 7% Syndecan4+ cells express PECAM-1 (H). Profiling simultaneously for three markers on live cells, we identified a subset of Syndecan-4+ cells that express the stem cell markers ABCG2 ([I], R11) and Sca1 ([J], R15). Approximately 7% of the hindlimb muscle-derived cells express both ABCG2 and Sca1 ([K], R19), and this subset of ABCG2+/Sca1+ cells represents ~3% of Syndecan-4+ cells ([L], R19). A satellite-SP cell (inset in [M] –[P]) in a 3D reconstruction of muscle section from a confocal Z series is located underneath the basal lamina ([M], red) and immunoreactive for ABCG2 ([N] and [P], cyan) and Syndecan-4 ([O] and [P], white). The inset (M–P) is a magnified region of the boxed area. (Q) A Venn diagram depicts the percentage of Syndecan-4+, ABCG2+, and dual positive cells represented in collagenase-digested hindlimb muscle. Freshly isolated myofibers retain rare satellite-SP cells ([R]–[U], caret) immunoreactive for ABCG2 ([R], red, caret), Sca1 ([S], green, caret), and Syndecan-4 ([T], white, caret); DNA is counterstained with DAPI ([R], [S], and [U], blue). In addition, note the ABCG2-negative Syndecan-4+ satellite cell on this fiber ([R]–[U], arrow), where DAPI is not bright in this plane of focus. In (B) and (D–H), black histograms represent specific antibody immunoreactivity, and gray histograms are the corresponding control. In (A)–(L), all gates were determined by setting controls at less than 0.5% positive events. For (M)–(P), the scale bar represents 75 μm, and for (R)–(U), 1 μm.

(8% of all dually positive satellite cells) express PECAM-1 (Figure 2H, Figure S1). We then profiled for three markers simultaneously—Syndecan-4, ABCG2, and Sca1, another stem cell marker previously identified on SP cells (Asakura et al., 2002; Jackson et al., 1999; Mitchell et al., 2005). As expected, the majority of ABCG2+ cells and Sca1+ cells are Syndecan-4− (Figure 2I, R10, and Figure 2J, R14, respectively). Consistent with the SP cell data (see Figure 1), we found that a population of Syndecan-4+ cells is immunoreactive for ABCG2 (Figure 2I, R11) and for Sca1 (Figure 2J, R15). The majority of ABCG2+ cells appear Sca1+ (Figure 2K, R19), and this ABCG2+/Sca1+ population is enriched in the ABCG2+/Syndecan-4+ cell population where virtually all Syndecan-4+/ABCG2+ cells are Sca1+ (Figure 2L, R19 compared to R21) and half of the Syndecan-4+/Sca1+ cells are ABCG2+ (Figure 2L, R18 compared to R19). This subset of satellite cells is rare, comprising 0.25% of the entire hindlimb mononuclear cell population (Figure 2Q), and averages between 3% and 10% of the Syndecan-4+ satellite cell population.

If these ABCG2+/Sca1+/Syndecan-4+ cells are satellite cells, they should reside in the satellite cell position in muscle sections and be retained on intact myofibers following myofiber isolation by enzymatic digestion. We found rare cells in the satellite cell position underneath the basal lamina (Figure 2M, inset) immunoreactive for Syndecan-4 and ABCG2 (Figures 2N–2P, inset). Some of these cells were found tightly associated with freshly isolated myofibers (Figures 2R–2U, carets). Although the percentages from the FACS profiles suggest that one to two Syndecan-4+/ABCG2+ SP cells are present on a typical myofiber (assuming ~25 satellite cells per myofiber), when fixed and stained we detect fewer cells than expected (0.5–1/myofiber), likely due to the low expression of ABCG2. These cells were also Sca1+ (Figure 2S, caret), strongly suggesting that they represent the cells observed by flow cytometry. Because these cells are present at the satellite cell position in skeletal muscle tissue, are found in the SP, express satellite cell markers, and remain tightly associated with myofibers during enzymatic isolation, we propose that these cells represent a subset of satellite cells and refer to this population as satellite-SP cells.

Satellite-SP Cells Express Pax7 and Have Distinct Behavior in Culture

The presence of satellite-SP cells on intact myofibers allows independent analysis of their behavior and comparison with the general satellite cell population in culture. Distinct from the major Syndecan-4+ population, where clusters of cells appear

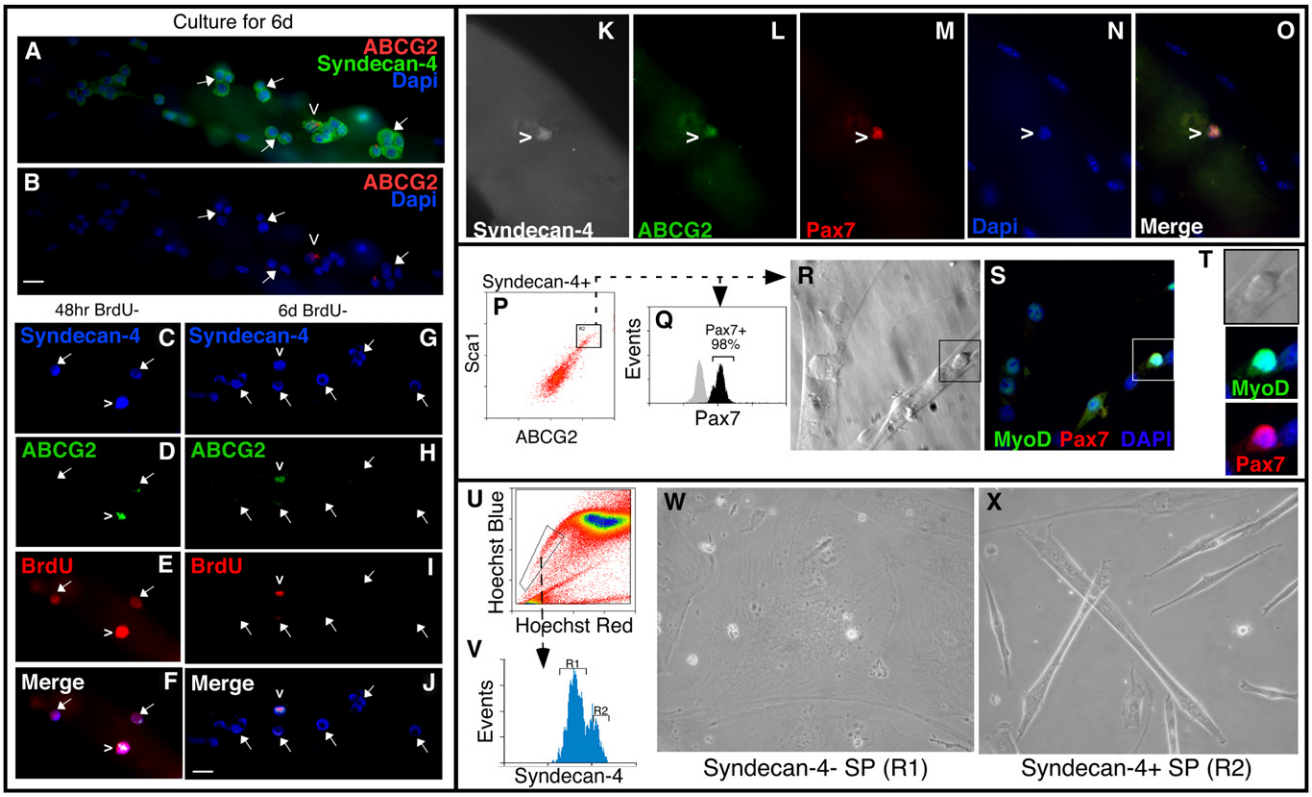

Figure 3. Satellite-SP Cells Express Pax7 and Exhibit Distinct Behaviors in Culture

Myofibers cultured for 6 days (A and B) retain single rare ABCG2+/Syndecan-4+ (red and green, respectively) satellite-SP cells (caret) surrounded by clusters of ABCG2-/Syndecan-4+ satellite cells (arrows mark some of the ABCG2–/Syndecan-4+ satellite cells). Following a 48 hr BrdU pulse and 48 hr chase, all satellite-SP cells ([C–F], caret) and satellite cells ([C–F], arrows) are BrdU positive (red, [C]–[F], Syndecan-4 [blue], and ABCG2 [green]). After a 6 day chase (G)–(J), only ABGG2+ satellite-SP cells (caret) retain BrdU (red), while satellite cells (arrows) are BrdU negative. Freshly isolated myofibers possess satellite-SP cells (caret in [K]–[O]) expressing Pax7 ([M], red) in addition to Syndecan-4 ([K], white) and ABCG2 ([L], green). FACS-sorted satellite-SP cells (P) were either fixed and permeabilized, demonstrating that all satellite-SP (Syndecan-4+/ABCG2+/Sca1+) cells are Pax7+ ([Q], black histogram), or cultured for 5 days, fixed, and visualized for myotubes (R) and stained for MyoD ([S], green) and Pax7 ([T], red). Boxed region in (R) and (S) identifies an unfused MyoD+/Pax7+ cell ([T], inset). Sorting muscle SP cells by Hoescht dye exclusion (U) for Syndecan-4 immunoreactivity ([V], R1 Syndecan-4− and R2 Syndecan-4+ muscle SP cells) followed by 3 weeks in culture (W and X) revealed that only Syndecan-4+ satellite-SP ([V], R2) cells spontaneously differentiated into myotubes (X). In (Q), the black histogram represents specific antibody immunoreactivity, and the gray histogram is the corresponding control. Scale bars represent 10 μm.

following 6 days in culture, single satellite-SP cells appear surrounded by Syndecan-4+ satellite cells (Figures 3A and 3B, caret marks satellite-SP cell). A number of possibilities could explain this observation, including (1) asymmetric cell division, (2) very slow cell cycling, (3) enhanced migration of the satellite-SP cells off of the myofibers, (4) enhanced cell death of satellite-SP cells, or (5) a failure of satellite-SP cells to divide in culture. The first two possibilities are not likely, as we did not observe satellite-SP cells on the tissue culture plates adjacent to the myofibers, nor did we observe apoptosis of satellite cells (data not shown). It is also possible that the ABCG2 immunoreactivity is lost during culture, and we cannot directly assess this possibility. To demonstrate cell-cycle entry of satellite-SP cells, we employed a BrdU pulse-chase assay, in which myofibers were cultured for the first 48 hr after harvest in the presence of BrdU followed by either a 48 hr or a 6 day chase in the absence of BrdU. Typically, Syndecan-4+ satellite cells on intact myofibers in culture will begin DNA synthesis 8–12 hr following isolation and undergo a synchronous division between 36 and 45 hr, with subsequent cell divisions occurring much more rapidly at 10–12 hr (our unpublished data). All satellite cells (Figures 3C–3F, arrows) and satellite-SP cells (Figures 3C–3F, carets) incorporate BrdU during the first 48 hr in culture and retain label 48 hr later, indicating that satellite-SP cells undergo a first cell division with kinetics roughly similar to Syndecan-4+ cells. However, following a 6 day chase in the absence of BrdU, Syndecan-4+ satellite cells continue to proliferate and dilute the BrdU label (Figures 3G–3J, arrows), whereas all satellite-SP cells retain BrdU, indicating that these cells cease cell division or cycle very slowly (Figures 3G–3J, caret). Curiously, we rarely observe ABCG2+/Syndecan-4+ doublets and typically find single isolated cells (Figures 3A–3J). If this is the result of asymmetric satellite-SP cell division giving rise to one daughter cell that retains the parental phenotype, the other daughter would be predicted to proliferate and thereby dilute the BrdU label. This is a possibility, since rare, asymmetric division of satellite cells has been observed (Kuang et al., 2007), and the expression of stem cell markers by the satellite-SP cells suggests that an asymmetric cell division event could explain the predominance of single satellite-SP cells.

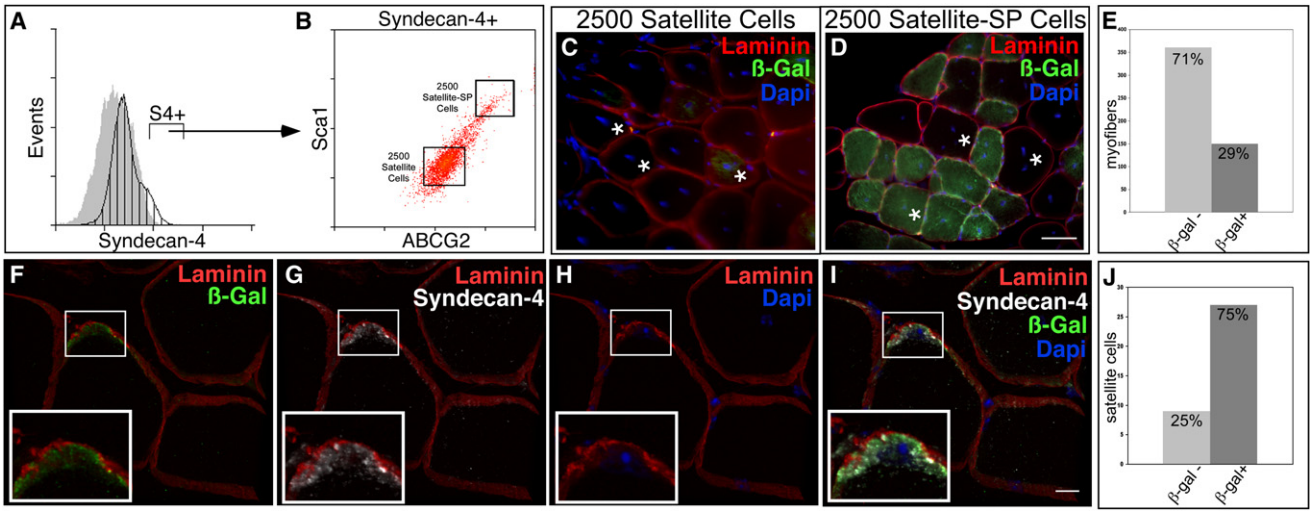

Figure 4. Satellite-SP Cells Engraft into Myofibers and the Satellite Cell Position In Vivo

(A and B) Hindlimb skeletal muscle from Rosa26 mice was sorted for satellite-SP cells (A), Syndecan-4+ ([B], Syndecan-4+/ABCG2+/Sca1+, top box), or satellite cells ([A], Syndecan-4+; [B], Syndecan-4+/ABCG2−/Sca1−, bottom box), and 2500 cells were transplanted into regenerating tibialis anterior muscle of different host mice with 1.2% $BaCl_2$.

(C and D) Representative epifluorescent images from cross-sections of transplanted and injured muscle depicting low numbers of β-galactosidase-expressing myofibers with transplantation of 2500 satellite cells (C) and β-galactosidase+ myofibers in satellite-SP cell transplanted tissue (D) 30 days after regeneration (asterisks mark centrally located nuclei).

(E) Scoring for donor-derived β-galactosidase+ myofibers following satellite-SP cell transplantation.

(F–I) 3D reconstruction of confocal images of donor-derived β-galactosidase+ ([F and I], green) satellite cells 30 days after transplantation of satellite-SP cells ([F–I], Laminin red; [G and I], Syndecan-4 white; [H and I], DAPI blue) with concurrent injury; insets are boxed. Scoring for donor-derived β-galactosidase+ satellite cells (J) 30 days after transplantation of satellite-SP cells. In (A), hatched histogram represents Syndecan-4, and gray histogram is the control; Syndecan-4+ (S4+) cells marked by bar. Scale bar in (D) represents 25 μm and in (I) represents 10 μm.

To further define the satellite cell character of satellite-SP cells, we asked if they express the paired box transcription factor Pax7, which is considered a marker of quiescent satellite cells and is required for satellite cell specification in vivo (Seale et al., 2000). Satellite-SP cells on intact myofibers that stain positive for Syndecan-4 (Figure 3K) and ABCG2 (Figure 3L) appear Pax7+ (Figures 3M and 3O). FACS-sorted satellite-SP cells (Figure 3P) were Syndecan-4+ and stained positive for Pax7 when cytospun (Figure S2); when analyzed by FACS, essentially all satellite-SP cells are Pax7+ (Figure 3Q), suggesting that these cells are committed to the myogenic lineage.

Satellite-SP cells express satellite cell markers and remain associated with myofibers, but we have not determined whether these cells are capable of spontaneous myogenic differentiation. In previous reports, skeletal muscle SP cells have not exhibited this potential and are only capable of initiating myogenesis when cocultured with satellite cells or skeletal muscle cell lines (Asakura et al., 2002). We reasoned that if satellite-SP cells were the only SP cells capable of myogenesis, then their myogenic phenotypes may have been overlooked in culture, since they represent only a small percentage of the muscle-derived SP population. Alternatively, myogenic commitment of muscle SP cells by coculture with myogenic cell lines may represent a required community effect. Therefore, we asked if satellite-SP cells are inherently myogenic in clonal cultures. FACS sorted satellite-SP cells cultured in growth media for 5 days differentiated into multinucleated myotubes (Figure 3R), whose nuclei express MyoD (Figure 3S) and retain mononuclear MyoD+/Pax7+ cells (Figures 3S and 3T, inset). As a further test to determine if satellite-SP cells, isolated by Hoechst dye exclusion, are capable of myogenesis, muscle SP cells were sorted into Syndecan-4+ and Syndecan-4− pools (Figures 3U and 3V), and the pools were individually cultured for 3 weeks in stem cell media. As expected, Syndecan-4− muscle SP cells fail to commit to a myogenic lineage (Figure 3W), while satellite-SP cells spontaneously differentiated and fused into multinucleated myotubes (Figure 3X). Thus, when isolated from the bulk of SP cells by dye exclusion or by FACS sorting, satellite-SP cells are capable of spontaneous myogenesis, supporting the hypothesis that these cells are capable of commitment to the myogenic lineage.

Satellite-SP Cells Are Myogenic Following Transplantation

If satellite-SP cells function as a myogenic progenitor or satellite stem cell, then we predict that they would produce satellite cell progeny capable of incorporation into the satellite cell niche as well as contributing myonuclei to myofibers. To address both the myogenic and stem cell capabilities of satellite-SP cells compared to satellite cells, we identified Syndecan-4+ cells by FACS from a Rosa26 (Zambrowicz et al., 1997) donor mouse to lineage mark cell progeny (Figure 4A), then sorted the Syndecan-4+ cells into two separate pools (Figure 4B), the satellite-SP cells (Syndecan-4+/ABCG2+/Sca1+) and satellite cells (Syndecan-4+/ABCG-/Sca1−). Tibialis anterior muscles of separate host mice were injected with 2500 satellite-SP cells or 2500 satellite cells in the presence of 1.2% $BaCl_2$ to induce muscle regeneration. The transplanted muscles were examined for donor cell

contribution 30 days following induced injury. Cross-sections from the satellite cell transplant show evidence of regeneration as indicated by centrally located nuclei (Figure 4C, asterisks), but there is little detectable donor cell engraftment into the myofibers and no detectable engraftment into the satellite cell niche (Figure 4C, data not shown). In satellite-SP transplanted muscle, β-galactosidase+ myofibers are numerous and clearly evident (Figures 4D and 4E), suggesting engraftment of donor satellite-SP cells. Moreover, β-galactosidase+ donor-derived cells (Figure 4F) that express Syndecan-4 (Figure 4G) were readily found in the host satellite cell niche located underneath the basal lamina (Figures 4F–4I), demonstrating that satellite cells as well as myonuclei can be derived from satellite-SP cell progeny in vivo. Satellite-SP cells contribute to myonuclei, as 30% of myofibers were β-galactosidase+ and thus contained donor-derived nuclei (Figure 4E, Table S2). The majority of these fibers possessed centrally located nuclei (Figure 4C, asterisk, Table S2), indicative of regenerated tissue. Transplantation of satellite cells produced few detectable β-galactosidase+ fibers (Figure 4C); however, we did find centrally located nuclei (Figure 4C, asterisk), affirming that the tissue was injured.

Engraftment of satellite-SP cells into the host tissue preferentially engrafts into the satellite cell niche, as demonstrated by the striking contribution of donor satellite cells to the regenerated tissue (Figure 4J). We found that 75% of all satellite cells present in the regenerated tibialis anterior muscle were donor-derived cells (Figure 4J, Table S3) as they engrafted into the satellite cell niche, were located underneath the basal lamina (Figures 4F–4I), and expressed the satellite cell marker Syndecan-4 (Figures 4G and 4I). The engraftment of satellite-SP cells demonstrates that they robustly and preferentially contribute to the satellite cell pool. Although we found β-galactosidase expression in myotubes, the capacity of the satellite-SP cells to differentiate into muscle in vivo is not addressed by these experiments. To determine if satellite-SP cells are capable of muscle differentiation, satellite-SP cells from a ROSA26 mouse were isolated by FACS as Syndecan-4+/ABCG2 +/Sca1+ and 2500 cells injected into the tibialis anterior muscle of an *mdx*^{4cv} mouse (Chapman et al., 1989) in the presence of $BaCl_2$ (Figures 5A and 5B). An examination of muscle sections 30 days following engraftment reveals extensive regeneration (Figure 5C, asterisks mark centrally located nuclei), extensive contribution of Dystrophin from the donor cells (Figure 5D), and localization of donor-contributed Dystrophin inside the basal lamina (Figures 5E and 5F). Contribution of engrafted satellite-SP cells to the myonuclear compartment in *mdx*^{4CV} was substantially greater than wild-type transplants, in which ~70% of the myofibers in the engrafted muscle were Dystrophin+ (Figure 5G, Table S4).

Engraftment of satellite-SP cells differed from engraftment of freshly isolated, CD34-enriched satellite cells, which require injection into irradiated, immunodeficient *mdx* mice (Montarras et al., 2005; Muskiewicz et al., 2005; Sacco et al., 2008) or diseased (*mdx*) mice (Cerletti et al., 2008). Thus, satellite-SP cells compete effectively with endogenous satellite cells since the host tissue is not irradiated to destroy the endogenous cells and injections are successful in wild-type regenerating muscle, not diseased muscle tissue, where endogenous satellite cells may be compromised. Together, our data show preferential engraftment of satellite-SP cells into the satellite cell niche with efficiencies not seen for any other cell types, suggesting the satellite-SP cell may function as a satellite stem cell. To provide further evidence in support of this hypothesis, we reinjured tibialis anterior muscles in *mdx*^{4CV} mice engrafted with 2500 satellite-SP cells from a ROSA26 mouse (Figures 6A–6C). Muscle sections were examined for the contribution of donor cells to the satellite cell and myonuclear compartments 30 days following reinjury. Similar to the primary engraftment, reinjured muscle shows extensive contribution of donor cells to the myonuclear compartment demonstrated by β-galactosidase+ myofibers (Figure 6D). Moreover, a large number of Syndecan-4+ cells are evident (Figure 6E) that are β-galactosidase+ (Figure 6F). A magnified 3D reconstruction from a confocal series shows a donor-derived satellite cell (Figure 6G, caret) and one endogenous satellite cell (Figure 6H, arrow) in reinjured muscle (Figure 6I). We tested the capacity of the donor-derived satellite cells in reinjured

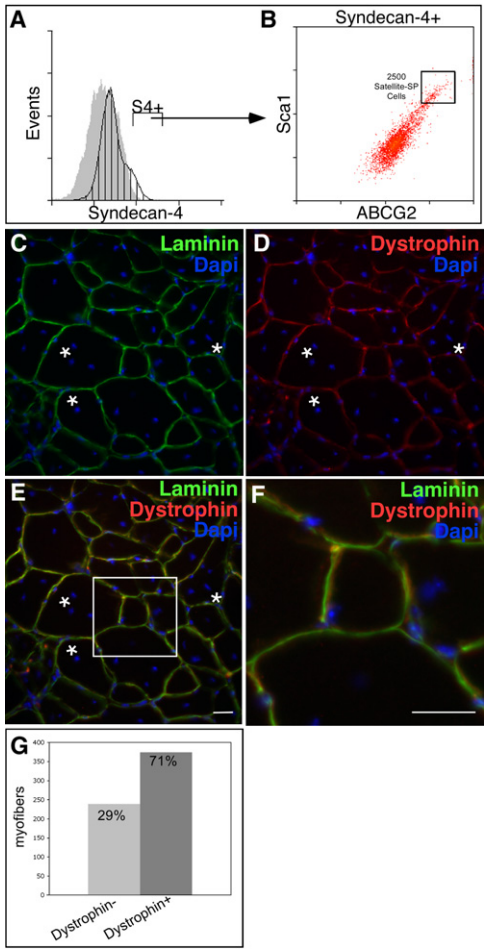

Figure 5. Satellite-SP Cells Generate Dystrophin+ Fibers Following Transplantation

Hindlimb skeletal muscle from Rosa26 mice was sorted for satellite-SP cells (A) and Syndecan-4+ ([B], Syndecan-4+/ ABCG2+/Sca1+, box) and transplanted into tibialis anterior muscles of *mdx*^{4cv} mice in the presence of 1.2% $BaCl_2$ to induce injury. (C–F) Representative epifluorescent images 30 days following transplantation and injury depicting centrally located nuclei (asterisks) and Dystrophin+ fibers ([D–F], red). Scoring is for Dystrophin+ fibers (G) 30 days following transplantation of satellite-SP cells.

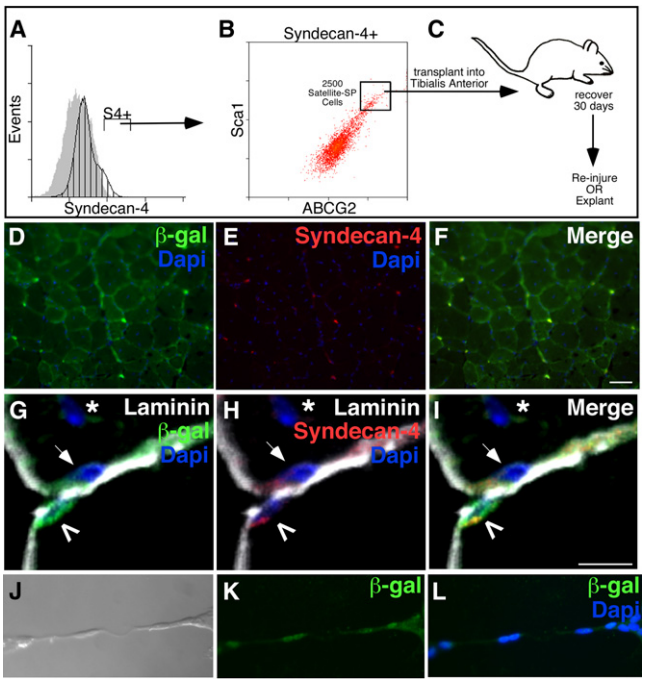

Figure 6. Transplanted Satellite-SP Cells Are Found after Multiple Rounds of Regeneration and Are Myogenic In Vitro

(A–C) Satellite-SP cells (A), Syndecan-4+ cells (B), and Syndecan-4+/ABCG2+/Sca1+ cells were isolated from hindlimb skeletal muscle of Rosa26 mice and transplanted into *mdx*^{4cv} tibialis anterior muscle. Following 30 days of regeneration, muscle was either reinjured with 1.2% $BaCl_2$ or explanted to isolate myofibers (C).

(D–F) Representative epifluorescent images of reinjured tissue with continued presence of donor-derived (β-galactosidase+, green [D and F]) Syndecan-4+ (red [E and F]) satellite cells.

(G–J) 3D reconstruction of confocal images of donor-derived (β-galactosidase+, green) Syndecan-4+ (red) cells located beneath the basal lamina (Laminin, white) 30 days following reinjury. Transplanted muscle fibers were were explanted, and satellite cells cultured and allowed to differentiate. Donor-derived, β-galactosidase+ (green [K and L]) cells formed myotubes.

mdx^{4CV} muscle to differentiate by explanting single myofibers, allowing the myofiber-associated cells to migrate off of the fiber into the culture dish. Donor-derived β-galactosidase+ cells differentiated and fused into multinucleated myotubes in culture (Figures 6J–6L), demonstrating the myogenic capacity of the satellite-SP cells following two successive rounds of muscle injury in the *mdx*^{4CV} mouse.

DISCUSSION

We have identified a subset of resident myogenic stem cells distinct from the majority of the satellite cell population that exhibit unique characteristics consistent with that of a satellite cell progenitor population. These cells express the satellite cell markers Pax7, Syndecan-3, and Syndecan-4; the SP marker ABCG2; and Sca1. They can be found in muscle sections and remain tightly associated with myofibers upon isolation. Whether isolated by dye exclusion or FACS sorted, these cells are capable of spontaneous differentiation into skeletal muscle. Unlike the majority of satellite cells, these cells possess an SP

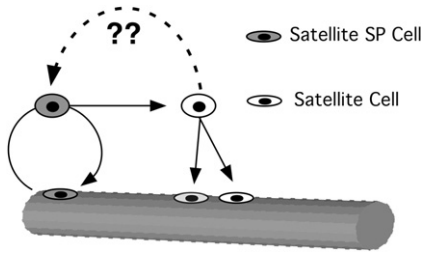

Figure 7. Satellite-SP Cells Self-Renew and Generate Satellite Cell Progeny

Satellite-SP cells (gray) may divide asymmetrically to produce a satellite-SP cell and a satellite cell. Satellite cells are capable of symmetric division to produce satellite cell progeny. It is not known if satellite-SP cells constitute a lineage or arise from the interaction of a satellite cell with a specialized niche.

phenotype identified by Hoechst dye exclusion, express ABCG2, and comprise ~3%–10% of the Syndecan-4+ population. When isolated, satellite-SP cells (Syndecan-4+/ABCG2+/Sca1+) exhibit a robust engraftment into the host satellite cell niche and generate myonuclear progeny that express muscle-specific genes. Moreover, upon reinjury, the contribution of donor-derived satellite-SP cells to the myonuclear and satellite cell compartments in reinjured muscle was equivalent or better than the initial engraftment, demonstrating the capacity of satellite-SP cells to renew the satellite cell pool. Whereas engraftment of CD34-enriched cells from muscle are capable of generating satellite cell progeny (Montarras et al., 2005; Cerletti et al., 2008; Sacco et al., 2008), satellite-SP cells are more efficient than any other reported cell type in generating satellite cell progeny when engrafted into host regenerating skeletal muscle. Moreover, satellite-SP cells appear capable of extensive self-renewal of the satellite cell pool in vivo, supporting our hypothesis that they function as satellite cell progenitors. Because these cells comprise a subpopulation of muscle SP cells, we believe that they may account for the variable myogenic capacity previously observed in cultures of muscle-derived SP cells (Asakura et al., 2002; Gussoni et al., 1999) and the satellite cell progenitor capacity observed in CD34-enriched satellite cells (Montarras et al., 2005; Cerletti et al., 2008; Sacco et al., 2008). Of particular interest is the observation that some of the skeletal muscle SP cells are somitically derived (Schienda et al., 2006), and it remains to be determined if the satellite-SP cells arise from this population. We propose a model (Figure 7) whereby satellite-SP cells function as myogenic progenitors or stem cells for the resident satellite cell population. Satellite-SP cells activate and divide to produce satellite cell progeny; we have not yet determined if satellite-SP cells constitute a distinct cell lineage or if a satellite-SP cell can arise from a main population satellite cell that is present in a specialized niche. The behavior of the satellite-SP cells in intact myofiber cultures suggests that the factors controlling their cell-cycle entry are distinct from those of the majority of satellite cells, since they appear to cycle once and then either exit the cell cycle completely or cycle very slowly, a trait that has been ascribed to both stem cells in general and myogenic stem cells in particular (Shinin et al., 2006; Conboy et al., 2007). Future work is aimed at identifying the factors necessary for satellite-SP cell proliferation, determining whether these cells generate satellite cell progeny

by an asymmetric division and identifying the source of satellite-SP cells.

EXPERIMENTAL PROCEDURES

Mice

Mice were bred and housed according to National Institutes of Health (NIH) guidelines for the ethical treatment of animals in a pathogen-free facility at the University of Colorado. Wild-type mice were C57Bl/6xDBA2 (B6D2F1; Jackson Labs); Rosa26 (B6;129S-*Gt(ROSA)26Sor*) (Zambrowicz et al., 1997) and *mdx*^{4CV} (Chapman et al., 1989) mice were obtained from Jackson Laboratory. *Abcg2/GFP* (Tadjali et al., 2006) mice were from Brian Sorrentino (St. Jude Children's Research Hospital). Cells or myofibers were harvested from female mice 3–6 months old.

Cells and Myofibers

Bone marrow cells were flushed from femurs and resuspended at 10^6 cells/ml in DMEM and 10% calf serum. Primary muscle cells were isolated from adult mouse hindlimb muscle. Briefly, muscle was digested with type I collagenase (Worthington), filtered, and recovered in F12-C and 15% horse serum and 0.5 nM FGF-2. SP cells were cultured in α-MEM media (Invitrogen) with 20% FBS and 0.5 nM FGF-2. Unless otherwise noted, myofibers and associated satellite cells were prepared as previously described (Cornelison et al., 2001) and either fixed immediately in 4% paraformaldehyde or cultured in F12-C and 15% horse serum and 0.5 nM FGF-2. As required, BrdU, at 10 μM (Sigma), was added.

FACS

For SP profiles, bone marrow cells and primary muscle cells were processed as described (Goodell et al., 1996). Briefly, following isolation, cells were incubated 90 min at 37°C in 5 μg/ml (bone marrow) or 7.5 μg/ml (muscle) Hoechst 33342 (Sigma). To delineate the SP gate, verapamil (Sigma) was added at a final concentration of 50 μM. Profiles/sorts were generated on a MoFlo cell sorter (DakoCytomation). For antibody staining, cells were incubated for 45 min at 4°C with primary antibodies (at 1:100 unless otherwise noted) as follows: mouse anti-ABCG2 (BCRP1) 5D3 (BD PharMingen), mouse anti-ABCG2-PE (BCRP1) 5D3 (Chemicon), rat anti-CD45-FITC 30-F11 (BD PharMingen), rat anti-Gr-1-Alexa488 RB6-8C5 (BoiLegend), rat anti-Mac-1-FITC M1/70 (Leinco Technologies), mouse anti-Pax7 (Developmental Studies Hybridoma Bank) conjugated to mouse Fc-PE-680 (Molecular Probes) at 1:5, rat anti-PECAM-FITC Mec13.3 (BD PharMingen), rat anti-Sca1-FITC E13-161.7 (BD PharMingen), rabbit anti-Syndecan-3 (Cornelison et al., 2001), chicken anti-Syndecan-4 (Cornelison et al., 2004) at 1:1500, and rat anti-Thy-1-FITC 30-H12 (BioLegend). Secondary antibodies were (at 1:100 unless otherwise noted) as follows: anti-chicken-Alexa488 (Molecular Probes) 1:500, anti-chicken-PE (Open Biosystems), anti-mouseIgG-PE-Cy5 (Santa Cruz), and anti-ratIgG-PE-Cy7 (Santa Cruz). Fluorescein diacetate (Sigma) was used at a final concentration of 2 μg/ml. Caltat fix and perm was used for permeabilized cells. Profiles/sorts were generated using the MoFlo (DakoCytomation) or FACScan (BD Biosciences) with background gates set such that secondary antibodies alone, or isotype controls, yielded fewer than 0.5% positive events.

Immunofluorescence

Cells, myofibers, and sections were fixed in 4% paraformaldehyde. In addition to the primary antibodies listed above, rabbit anti-galactosidase (Abcam, 1:1000), rat anti-BrdU BU1/75 (Serotec, 1:100), rabbit anti-Dystrophin (Abcam, 1:200), rat anti-laminin 4HB-2 (Sigma, 1:200), and rabbit anti-laminin (Sigma, 1:200) were used. Additional secondary antibodies were as follows: anti-chicken-Alexa594 or 647 (Molecular Probes); anti-chicken-AMCA (Jackson ImmunoResearch); anti-mouse-Alexa488 or 594 (Molecular Probes); anti-mouseIgG$_1$-FITC (SouthernBiotech); anti-mouseIgG$_{2b}$-Texas Red (SouthernBiotech); anti-rat-Alexa488, -594, or -647 (Molecular Probes); anti-rat-AMCA (Jackson ImmunoResearch); and anti-rabbit-Alexa488, -594, or -647 (Molecular Probes), all at 1:100, except Alexa probes were at 1:500. Epifluorescent images were captured using a Nikon Eclipse E800 equipped with a Cooke Sensicam digital camera and deconvoluted using Slidebook software (Intelligent Imaging Innovations). Deconvoluted background fluorescence was subtracted from the primary signal. Individual tiff files were exported from Slidebook software. Confocal images and Z series stacks were captured with a Leica TCS SP2 AOBS confocal microscope. Fluorescent images were processed with either Leica software or Volocity (Improvision) to process 3D reconstructions.

Microarray

Cells were isolated from mouse hindlimb muscle and sorted for Syndecan-3/Syndecan-4 expression as described above; source muscles were either uninjured or injected with 1.2% $BaCl_2$ 24 hr prior to harvest to induce myonecrosis (Caldwell et al., 1990). At least three independent age-matched animals were analyzed per time point. Total RNA was isolated using a PicoPure RNA Isolation Kit (Arcturus) followed by two rounds of linear T7-based amplification (RiboAmp HA Kit, Arcturus) for an RNA equivalent to 5000 dual-positive cells (based on the number of cells collected). Biotin-labeled antisense RNA was generated with IVT Labeling Kit (Affymetrix), and labeled cRNA was quantified and analyzed for size representation using a BioAnalyzer (Agilent). Labeled cRNA (5 μg) was fragmented and hybridized to Affymetrix 430 v.2 mouse microarrays at the University of Colorado Core facilities; chips were scanned on a GeneChip Scanner 3000 (Affymetrix) and intensity data recovered in GCOS (Affymetrix). CEL files from three replicate genechips were imported directly into Spotfire (TIBCO) and normalized by GCRMA. ANOVA analysis set at an FDR of 0.05% was used to identify differentially expressed probe sets. Probe sets with ≥2-fold changes between uninjured and 24 hr injured data sets were further identified by K-means and SOM clustering. Probe sets with significant changes observed in satellite and stem cells were identified and plotted according to their relative expression.

Regeneration and Cell Transplants

To isolate cells from injured tissue, mice were anesthetized with isoflurane, and tibialis anterior muscles were injected with 50 μl 1.2% $BaCl_2$, followed with a 24 hr recovery period. Muscles were processed for sorting and RNA extraction as described above. For transplantation studies, donor Syndecan-4+/ABCG2+/Sca1+ and Syndecan-4+/ABCG2−/Sca1− cells were isolated from hindlimb muscles of Rosa26 mice. Host B6D2F1 mice were anesthetized with isoflurane, and tibialis anterior muscles were injected with donor cells in 50 μl 1.2% $BaCl_2$ followed with recovery periods of 30 days. Muscle tissue was then harvested and processed for immunofluorescence as described above.

SUPPLEMENTAL DATA

The Supplemental Data include four tables, two figures, and Supplemental References and can be found with this article online at http://www.cell.com/cell-stem-cell/supplemental/S1934-5909(09)00019-8.

ACKNOWLEDGMENTS

The authors would like to acknowledge Karen Helm at The University of Colorado Cancer Center Flow Cytometry Core (supported by NIH P30CA046934) for assistance with cell isolation and Helen Marshall at the University of Colorado, MCD-Biology Department DNA Array Analysis Facility for Affymetrix hybridization and scanning. This work was supported by NIH AR39467, AR49446, AG28907, and a grant from the Muscular Dystrophy Association to B.B.O.; NIH 5T32HL007851 to K.K.T.; Muscular Dystrophy Association Development Grant to D.D.W.C.; NIH GM066728-01 to J.K.H.; and APS Giles Filley Award and AHA-SDG0335032N to S.M.M.

Received: June 29, 2008
Revised: December 3, 2008
Accepted: January 21, 2009
Published: March 5, 2009

REFERENCES

Asakura, A., Seale, P., Girgis-Gabardo, A., and Rudnicki, M.A. (2002). Myogenic specification of side population cells in skeletal muscle. J. Cell Biol. *159*, 123–134.

Asakura, A., Hirai, H., Kablar, B., Morita, S., Ishibashi, J., Piras, B.A., Christ, A.J., Verma, M., Vineretsky, K.A., and Rudnicki, M.A. (2007). Increased survival of muscle stem cells lacking the MyoD gene after transplantation into regenerating skeletal muscle. Proc. Natl. Acad. Sci. USA *104*, 16552–16557.

Beauchamp, J.R., Morgan, J.E., Pagel, C.N., and Partridge, T.A. (1999). Dynamics of myoblast transplantation reveal a discrete minority of precursors with stem cell-like properties as the myogenic source. J. Cell Biol. *144*, 1113–1122.

Bosnakovski, D., Xu, Z., Li, W., Thet, S., Cleaver, O., Perlingeiro, R.C., and Kyba, M. (2008). Prospective isolation of skeletal muscle stem cells with a Pax7 reporter. Stem Cells *26*, 3194–3204.

Brack, A.S., Conboy, M.J., Roy, S., Lee, M., Kuo, C.J., Keller, C., and Rando, T.A. (2007). Increased Wnt signaling during aging alters muscle stem cell fate and increases fibrosis. Science *317*, 807–810.

Caldwell, C.J., Mattey, D.L., and Weller, R.O. (1990). Role of the basement membrane in the regeneration of skeletal muscle. Neuropathol. Appl. Neurobiol. *16*, 225–238.

Cerletti, M., Jurga, S., Witczak, C.A., Hirshman, M.F., Shadrach, J.L., Goodyear, L.J., and Wagers, A.J. (2008). Highly efficient, functional engraftment of skeletal muscle stem cells in dystrophic muscles. Cell *134*, 37–47.

Chapman, V.M., Miller, D.R., Armstrong, D., and Caskey, C.T. (1989). Recovery of induced mutations for X chromosome-linked muscular dystrophy in mice. Proc. Natl. Acad. Sci. USA *86*, 1292–1296.

Conboy, M.J., Karasov, A.O., and Rando, T.A. (2007). High incidence of non-random template strand segregation and asymmetric fate determination in dividing stem cells and their progeny. PLoS Biol. *5*, e102. 10.1371/journal.pbio.0050102.

Cornelison, D., Filla, M.S., Stanley, H.M., Rapraeger, A.C., and Olwin, B.B. (2001). Syndecan-3 and syndecan-4 specifically mark skeletal muscle satellite cells and are implicated in satellite cell maintenance and muscle regeneration. Dev. Biol. *239*, 79–94.

Cornelison, D.D., Wilcox-Adelman, S.A., Goetinck, P.F., Rauvala, H., Rapraeger, A.C., and Olwin, B.B. (2004). Essential and separable roles for Syndecan-3 and Syndecan-4 in skeletal muscle development and regeneration. Genes Dev. *18*, 2231–2236.

De Angelis, L., Berghella, L., Coletta, M., Lattanzi, L., Zanchi, M., Cusella-De Angelis, M.G., Ponzetto, C., and Cossu, G. (1999). Skeletal myogenic progenitors originating from embryonic dorsal aorta coexpress endothelial and myogenic markers and contribute to postnatal muscle growth and regeneration. J. Cell Biol. *147*, 869–878.

Dellavalle, A., Sampaolesi, M., Tonlorenzi1, R., Tagliafico, E., Sacchetti, B., Perani, L., Innocenzi, A., Galvez, B.G., Messina, G., Morosetti, R., et al. (2007). Pericytes of human skeletal muscle are myogenic precursors distinct from satellite cells. Nat. Cell Biol. *9*, 255–267.

Goodell, M.A., Brose, K., Paradis, G., Conner, A.S., and Mulligan, R.C. (1996). Isolation and functional properties of murine hematopoietic stem cells that are replicating in vivo. J. Exp. Med. *183*, 1797–1806.

Gussoni, E., Soneoka, Y., Strickland, C.D., Buzney, E.A., Khan, M.K., Flint, A.F., Kunkel, L.M., and Mulligan, R.C. (1999). Dystrophin expression in the mdx mouse restored by stem cell transplantation. Nature *401*, 390–394.

Jackson, K.A., Mi, T., and Goodell, M.A. (1999). Hematopoietic potential of stem cells isolated from murine skeletal muscle. Proc. Natl. Acad. Sci. USA *96*, 14482–14486.

Kuang, S., Kuroda, K., Le Grand, F., and Rudnicki, M.A. (2007). Asymmetric self-renewal and commitment of satellite stem cells in muscle. Cell *129*, 999–1010.

LaBarge, M.A., and Blau, H.M. (2002). Biological progression from adult bone marrow to mononucleate muscle stem cell to multinucleate muscle fiber in response to injury. Cell *111*, 589–601.

Majka, S.M., Jackson, K.A., Kienstra, K.A., Majesky, M.W., Goodell, M.A., and Hirschi, K.K. (2003). Distinct progenitor populations in skeletal muscle are bone marrow derived and exhibit different cell fates during vascular regeneration. J. Clin. Invest. *111*, 71–79.

Majka, S.M., Beutz, M.A., Hagen, M., Izzo, A.A., Voelkel, N., and Helm, K.M. (2005). Identification of novel resident pulmonary stem cells: form and function of the lung side population. Stem Cells *23*, 1073–1081.

Meeson, A.P., Hawke, T.J., Graham, S., Jiang, N., Elterman, J., Hutcheson, K., Dimaio, J.M., Gallardo, T.D., and Garry, D.J. (2004). Cellular and molecular regulation of skeletal muscle side population cells. Stem Cells *22*, 1305–1320.

Mitchell, P.O., Mills, T., O'Connor, R.S., Kline, E.R., Graubert, T., Dzierzak, E., and Pavlath, G.K. (2005). Sca-1 negatively regulates proliferation and differentiation of muscle cells. Dev. Biol. *283*, 240–252.

Montanaro, F., Liadaki, K., Schienda, J., Flint, A., Gussoni, E., and Kunkel, L.M. (2004). Demystifying SP cell purification: viability, yield, and phenotype are defined by isolation parameters. Exp. Cell Res. *298*, 144–154.

Montarras, D., Morgan, J., Collins, C., Relaix, F., Zaffran, S., Cumano, A., Partridge, T., and Buckingham, M. (2005). Direct isolation of satellite cells for skeletal muscle regeneration. Science *309*, 2064–2067.

Muskiewicz, K.R., Frank, N.Y., Flint, A.F., and Gussoni, E. (2005). Myogenic potential of muscle side and main population cells after intravenous injection into sub-lethally irradiated mdx mice. J. Histochem. Cytochem. *53*, 861–873.

Olguin, H.C., and Olwin, B.B. (2004). Pax-7 up-regulation inhibits myogenesis and cell cycle progression in satellite cells: a potential mechanism for self-renewal. Dev. Biol. *275*, 375–388.

Sacco, A., Doyonnas, R., Kraft, P., Vitorovic, S., and Blau, H.M. (2008). Self-renewal and expansion of single transplanted muscle stem cells. Nature *456*, 502–506.

Sampaolesi, M., Torrente, Y., Innocenzi, A., Tonlorenzi, R., D'Antona, G., Pellegrino, M.A., Barresi, R., Bresolin, N., De Angelis, M.G., Campbell, K.P., et al. (2003). Cell therapy of alpha-sarcoglycan null dystrophic mice through intra-arterial delivery of mesoangioblasts. Science *301*, 487–492.

Sampaolesi, M., Blot, S., D'Antona, G., Granger, N., Tonlorenzi, R., Innocenzi, A., Mognol, P., Thibaud, J.L., Galvez, B.G., Barthélémy, I., et al. (2006). Mesoangioblast stem cells ameliorate muscle function in dystrophic dogs. Nature *444*, 574–579.

Schienda, J., Engleka, K.A., Jun, S., Hansen, M.S., Epstein, J.A., Tabin, C.J., Kunkel, L.M., and Kardon, G. (2006). Somitic origin of limb muscle satellite and side population cells. Proc. Natl. Acad. Sci. USA *103*, 945–950.

Schultz, E. (1996). Satellite cell proliferative compartments in growing skeletal muscles. Dev. Biol. *175*, 84–94.

Seale, P., Sabourin, L.A., Girgis-Gabardo, A., Mansouri, A., Gruss, P., and Rudnicki, M.A. (2000). Pax7 is required for the specification of myogenic satellite cells. Cell *102*, 777–786.

Shinin, V., Gayraud-Morel, B., Gomès, D., and Tajbakhsh, S. (2006). Asymmetric division and cosegregation of template DNA strands in adult muscle satellite cells. Nat. Cell Biol. *8*, 677–682.

Tadjali, M., Zhou, S., Rehg, J., and Sorrentino, B.P. (2006). Prospective isolation of murine hematopoietic stem cells by expression of an Abcg2/GFP allele. Stem Cells *24*, 1556–1563.

Zambrowicz, B.P., Imamoto, A., Fiering, S., Herzenberg, L.A., Kerr, W.G., and Soriano, P. (1997). Disruption of overlapping transcripts in the ROSA beta geo 26 gene trap strain leads to widespread expression of beta-galactosidase in mouse embryos and hematopoietic cells. Proc. Natl. Acad. Sci. USA *94*, 3789–3794.

Zammit, P.S., Golding, J.P., Nagata, Y., Hudon, V., Partridge, T.A., and Beauchamp, J.R. (2004). Muscle satellite cells adopt divergent fates: a mechanism for self-renewal? J. Cell Biol. *166*, 347–357.

Zhou, S., Schuetz, J.D., Bunting, K.D., Colapietro, A.M., Sampath, J., Morris, J.J., Lagutina, I., Grosveld, G.C., Osawa, M., Nakauchi, H., and Sorrentino, B.P. (2001). The ABC transporter Bcrp1/ABCG2 is expressed in a wide variety of stem cells and is a molecular determinant of the side-population phenotype. Nat. Med. *7*, 1028–1034.